JCI The Journal of Clinical Investigation

Amendment history:
- Corrigendum (December 1999)

Dilated cardiomyopathy in homozygous myosin-binding protein-C mutant mice

Bradley K. McConnell, … , Christine E. Seidman, J.G. Seidman

J Clin Invest. 1999;104(9):1235-1244. https://doi.org/10.1172/JCI7377.

Article

To elucidate the role of cardiac myosin-binding protein-C (MyBP-C) in myocardial structure and function, we have produced mice expressing altered forms of this sarcomere protein. The engineered mutations encode truncated forms of MyBP-C in which the cardiac myosin heavy chain-binding and titin-binding domain has been replaced with novel amino acid residues. Analogous heterozygous defects in humans cause hypertrophic cardiomyopathy. Mice that are homozygous for the mutated MyBP-C alleles express less than 10% of truncated protein in M-bands of otherwise normal sarcomeres. Homozygous mice bearing mutated MyBP-C alleles are viable but exhibit neonatal onset of a progressive dilated cardiomyopathy with prominent histopathology of myocyte hypertrophy, myofibrillar disarray, fibrosis, and dystrophic calcification. Echocardiography of homozygous mutant mice showed left ventricular dilation and reduced contractile function at birth; myocardial hypertrophy increased as the animals matured. Left-ventricular pressure-volume analyses in adult homozygous mutant mice demonstrated depressed systolic contractility with diastolic dysfunction. These data revise our understanding of the role that MyBP-C plays in myofibrillogenesis during cardiac development and indicate the importance of this protein for long-term sarcomere function and normal cardiac morphology. We also propose that mice bearing homozygous familial hypertrophic cardiomyopathy–causing mutations may […]

Dilated cardiomyopathy in homozygous myosin-binding protein-C mutant mice

Bradley K. McConnell,[1] Karen A. Jones,[1] Diane Fatkin,[2] Luis H. Arroyo,[3] Richard T. Lee,[3] Orlando Aristizabal,[4] Daniel H. Turnbull,[4] Dimitrios Georgakopoulos,[5] David Kass,[5] Meredith Bond,[6] Hideshi Niimura,[1] Frederick J. Schoen,[7] David Conner,[1] Donald H. Fischman,[8] Christine E. Seidman,[2] and J.G. Seidman[1]

[1]Department of Genetics, Howard Hughes Medical Institute and Harvard Medical School, Boston, Massachusetts 02115, USA
[2]Cardiovascular Division and Howard Hughes Medical Institute, Brigham and Women's Hospital, Boston, Massachusetts 02115, USA
[3]Cardiovascular Division, Department of Medicine, Brigham and Women's Hospital, Boston, Massachusetts 02115, USA
[4]Skirball Institute of Biomolecular Medicine, New York University School of Medicine, New York, New York 10016, USA
[5]Division of Cardiology, The Johns Hopkins Medical Institute, Baltimore, Maryland 21287, USA
[6]Department of Molecular Cardiology, Lerner Research Institute, The Cleveland Clinic Foundation, Cleveland, Ohio 44195, USA
[7]Department of Pathology, Brigham and Women's Hospital, Boston, Massachusetts 02115, USA
[8]Department of Cell Biology, Weill Medical College of Cornell University, New York, New York 10021, USA

Address correspondence to: Jonathan Seidman, Department of Genetics, Harvard Medical School, 200 Longwood Avenue, Alpert Building, Boston, Massachusetts 02115, USA.
Phone: (617) 432-7871; Fax: (617) 432-7832; E-mail: seidman@rascal.med.harvard.edu.

Bradley K. McConnell and Karen A. Jones contributed equally to this work.

Received for publication May 19, 1999, and accepted in revised form September 28, 1999.

To elucidate the role of cardiac myosin-binding protein-C (MyBP-C) in myocardial structure and function, we have produced mice expressing altered forms of this sarcomere protein. The engineered mutations encode truncated forms of MyBP-C in which the cardiac myosin heavy chain-binding and titin-binding domain has been replaced with novel amino acid residues. Analogous heterozygous defects in humans cause hypertrophic cardiomyopathy. Mice that are homozygous for the mutated MyBP-C alleles express less than 10% of truncated protein in M-bands of otherwise normal sarcomeres. Homozygous mice bearing mutated MyBP-C alleles are viable but exhibit neonatal onset of a progressive dilated cardiomyopathy with prominent histopathology of myocyte hypertrophy, myofibrillar disarray, fibrosis, and dystrophic calcification. Echocardiography of homozygous mutant mice showed left ventricular dilation and reduced contractile function at birth; myocardial hypertrophy increased as the animals matured. Left-ventricular pressure-volume analyses in adult homozygous mutant mice demonstrated depressed systolic contractility with diastolic dysfunction. These data revise our understanding of the role that MyBP-C plays in myofibrillogenesis during cardiac development and indicate the importance of this protein for long-term sarcomere function and normal cardiac morphology. We also propose that mice bearing homozygous familial hypertrophic cardiomyopathy–causing mutations may provide useful tools for predicting the severity of disease that these mutations will cause in humans.

J. Clin. Invest. **104**:1235–1244 (1999).

Introduction

Hypertrophic and dilated cardiomyopathies are important pathologies that increase myocardial mass, albeit with distinct patterns of remodeling (reviewed in refs. 1, 2). Hypertrophic cardiomyopathy produces ventricular wall thickening without increases in ventricular volume, whereas both wall thickness and chamber volumes increase in dilated cardiomyopathy. Contractile parameters further discriminate between these pathologies, with systolic function preserved or improved in hypertrophic hearts but diminished in dilated cardiomyopathy. Whereas the triggering events for each of these pathologies usually appear to be different, clinical observations indicate a potential overlap in the molecular signals and/or cellular events that remodel the heart, because some patients with hypertrophic cardiomyopathy develop a dilated phenotype.

Mutations in cardiac myosin-binding protein-C (MyBP-C) account for approximately 20% of familial hypertrophic cardiomyopathy (FHC) (3–7). Whereas mutations of other sarcomere proteins that participate in force generation are expected to cause FHC by a dominant negative effect on contractile properties, the mechanism(s) by which cardiac MyBP-C defects cause FHC are less certain (reviewed in refs. 8, 9). MyBP-C is a large and abundant myofibrillar protein with both structural and regulatory functions (10). During cardiac development, MyBP-C expression corresponds to the onset of myofibrillogenesis, and 3 fibronectin-like motifs are thought to be necessary for thick filament

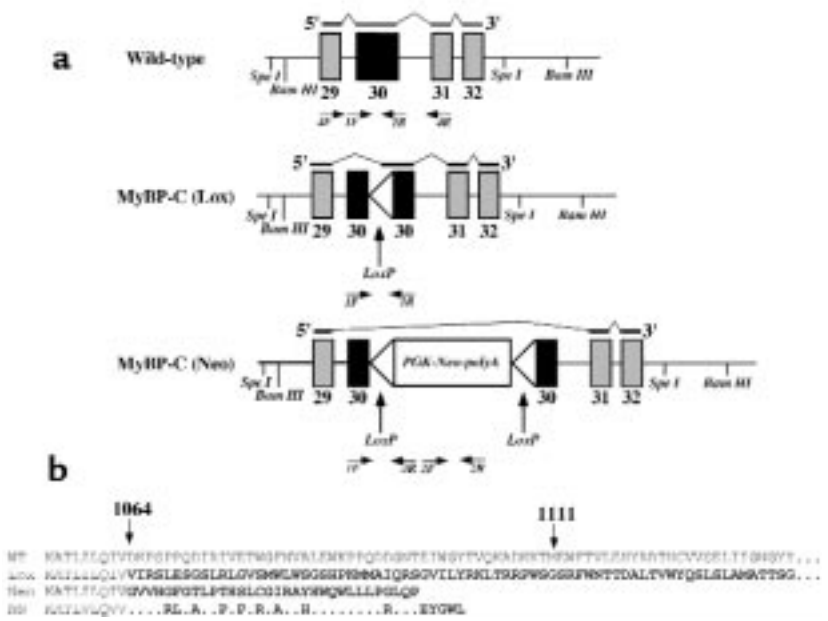

Figure 1
Schematic of (**a**) the genomic structure of *wild-type MyBP-C*, *MyBP-C(LoxP)*, and *MyBP-C(Neo)* alleles, the RNAs produced by each allele, and (**b**) the structure of the MyBP-C proteins encoded by each allele. (**a**) Exons 29–32 of the murine cardiac MyBP-C gene are shown for each allele (see Methods). The mutations alter only exon 30; all other exons are identical. The black lines above each gene segment reflect the structure of the encoded RNA indicated in the 5′→3′ orientation; thick lines are exons incorporated into the RNA, thin lines indicate skipped segments of the gene not found in RNA. The genotypes of mice were determined with primers 1F, 1R, 2F, 2R, and 3R. Primers 4F and 4R were used to determine the structure of MyBP-C RNA; structures of the deduced RNAs are indicated above each allele. (**b**) The structure of carboxyl ends of the MyBP-C polypeptides encoded by *MyBP-C(Neo)* and *MyBP-C(Lox)* alleles were deduced from the sequences of RNA found in the left ventricles of homozygous mice bearing the indicated allele. The residues (between residues 1064 and 1111) of the wild-type protein are encoded by exon 30. Novel amino acid residues at the carboxyl end of the mutant proteins (bold) are encoded by altered reading of exon 30 (Lox) or exon 31 (Neo). The wild-type MyBP-C protein is 1270 amino acids whereas the MyBP-C(Lox) protein is 1240-amino acids long; the complete sequences of these 2 carboxyl ends are not shown. The carboxyl end of the analogous human mutation found in family NN (3) is shown for comparison. Differences between the family NN protein and the MyBP-C(Neo) protein reflect sequence differences between the mouse and human MyBP-C gene exon 31.

assembly. In the mature heart, MyBP-C is found in 7–9 transverse strips (spaced about 43 nm apart) located in the C-zone of sarcomere A-bands (11–13). Whereas MyBP-C does not directly participate in force generation, reversible phosphorylation by cAMP-dependent protein kinase A (14) and calcium/calmodulin-dependent protein kinase II (15) may affect contractile function by stimulating cardiac actomyosin ATPase (16) or influencing myofibril tension generation and contractile velocity (17). Six FHC-causing MyBP-C mutations that are predicted to encode truncated polypeptides (3–5) that lack carboxyl residues required to bind myosin heavy chain and titin and that have novel residues at their carboxyl termini have been described. FHC is an autosomal dominant trait, and affected individuals are heterozygous for these mutations. Individuals bearing these 6 FHC-causing mutations have clinically similar forms of FHC. The mechanism by which FHC-causing MyBP-C mutations perturb cardiac structure and function is unknown, because neither mutant peptides nor reduced levels of MyBP-C has been found in cardiac tissue from affected patients (18).

We have created mice bearing a mutationally altered murine cardiac MyBP-C gene that encodes a truncated peptide, analogous to that found in human hypertrophic cardiomyopathy. Although FHC patients are heterozygous, bearing 1 mutant and 1 wild-type MyBP-C allele, we have bred the mice bearing mutant MyBP-C alleles to homozygosity so that they carry only mutated MyBP-C alleles. Normal MyBP-C protein cannot be expressed in cardiac tissues of these mice, and mutant MyBP-C peptides are found at markedly reduced levels. We hypothesized that homozygous mice bearing mutant MyBP-C alleles might have a different cardiac phenotype than heterozygous mice bearing a single mutant allele and a single wild-type allele. We have studied cardiac structure and function of the homozygous mutant mice to better define the mechanisms by which FHC-causing MyBP-C mutations alter cardiac physiology.

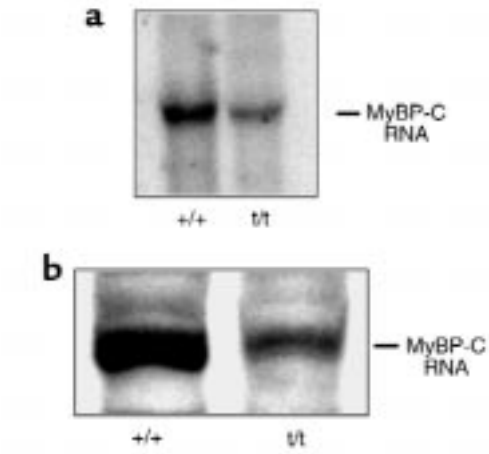

Figure 2
MyBP-C mRNA and protein expression levels in hearts of 12-week-old homozygous MyBP-C(Neo) mice (designated t/t). (**a**) Northern blot analyses of RNAs from left ventricle of wild-type (+/+) and MyBP-C(Neo) mice hybridized with murine MyBP-C and GAPDH probes. (**b**) Western blot analyses identified the 150-kDa MyBP-C protein in myofibrillar extracts of the LV of wild-type (+/+) and homozygous MyBP-C(Neo) mice (t/t).

Methods

Generation of homozygous mutant cardiac MyBP-C mice. Murine MyBP-C sequences were amplified from cardiac RNA by RT-PCR using oligonucleotide primers 3301F and 3900R derived from the published human *MYBPC3* gene sequence (EMBL accession number X84075) and used to probe a 129SvJ sub-genomic library (unpublished). A bacteriophage clone, λMyBPc, containing the murine MyBP-C gene was isolated, from which a 7.4-kb *Spe*I fragment was subcloned into pBluescript and characterized by partial nucleotide sequence analysis. Intron-exon boundaries were deduced by comparison with the human gene (Figure 1a). A blunt-ended, 2-kb fragment encoding the neomycin gene flanked by *LoxP* sequences was excised from plasmid *pPTloxPNeo* (kindly provided by J. Rossant), and inserted into the *Eco*RV site within exon 30.

The targeting construct was introduced into embryonic stem (ES) cells and selected (19). Colonies were screened for homologous recombination by Southern blot analyses using an external probe (data not shown). Targeted ES cells were injected into mouse blastocysts as described (20). Genotypes were ascertained from tail DNA in the offspring of chimeric animals by PCR analyses (25 μL assay) using primers (Figure 1a) to amplify exon 30: 1F (CTAGGTACTAACAG GCTCCTGCTT), 1R (CCTACCATGCAGGAAACCAGAATA) and primers: 2F (GGTTCTTTTT GTCAAGACCGAC), 2R (GTAGCCGGATCAAGCGTATG) to amplify the inserted neomycin cassette.

In addition a male chimeric mouse was mated with an EIIa-Cre transgenic mouse (kindly provided by H. Westphal, National Institutes of Health, Bethesda, Maryland, USA; ref. 21) to produce progeny in which the *LoxP*-flanked *Neo* gene had been efficiently deleted (Figure 1a). The MyBP-C (Lox) genotype was determined by PCR analyses of exon 30 and absence of Neo sequences. Mice homozygous for the *MyBP-C(Neo)* or *MyBP-C(Lox)* alleles (both designated MyBP-C$^{t/t}$) were produced by breeding heterozygous animals.

RNA analyses. Total RNA was isolated from left ventricle (LV), right ventricle (RV), and atrium, using Trizol (GIBCO BRL Life Technologies, Frederick, Maryland, USA) and analyzed by standard Northern blot procedures (22). MyBP-C RNA was detected using a ^{32}P-labeled insert from a mouse cDNA clone designated pcMyBPC, which encodes MyBP-C amino acid residues 582–1110. Other RNAs were detected using 5′-^{32}P-labeled transcript-specific oligonucleotide probes with standard hybridization conditions (23) as follows: α-skeletal actin: 5′-TGGCTTTAATGCTTCAAGTTTT CATTTCCTTTCCACAGGG; brain natriuretic peptide (BNP): 5′-CAGCTTGAGATATGTGTCACCTTGGAATTTTGAGGTCTCT GCTGGACC; sarcoplasmic reticulum Ca^{2+}-ATPase (SERCA): 5′-AACAACGCACATGCACGCACCCGAACAC CTTATATTTCTGCAAATGG; GAPDH: 5′-GGAA-CATGTAGACCATGTAGTTGAGGTCAATGAAG. Hybridization signals were quantified using ImageQuant software (Molecular Dynamics, Sunnyvale, California, USA), and normalized to the signal intensity observed with an oligonucleotide specific for GAPDH RNA. Student's *t* tests were performed to determine whether the data were significantly different between the groups of mice.

The structure of MyBP-C RNA was assessed by nucleotide sequence analysis of RT-PCR–amplified DNA fragments using conditions described previously (3) with primers 4F (TCAGGTGACCTGGACCAAAGAG) and 4R (ATGTTATGGCTGAAGACCCGG).

Protein analyses. Cardiac tissues were isolated, washed in Dulbecco's PBS, blotted on filter paper, and homogenized in ice-cold inhibiting buffer (24) containing 50 mM potassium dihydrogen phosphate (KH_2PO_4), 70 mM sodium fluoride (NaF), and 5 mM EDTA, with protease inhibitors (5 μg/mL antipain, 10 μg/mL leupeptin, 5 μg/mL pepstatin A, 43 μg/mL PMSF, 5 mM EGTA, and 0.1 μM sodium orthovanadate). Myofibrillar fractions were isolated from total protein homogenates by centrifugation at 15,000 *g* for 5 minutes at 4°C. The pellet was resuspended in inhibiting buffer plus 1% Triton X-100. Detergent-extracted myofibrils were again centrifuged at 5000 *g* for 5 minutes, and the pellet was resuspended in inhibiting buffer.

Table 1
Left ventricular dimensions of wild-type and homozygous mutant MyBP-C mice

Genotype[A]	Body wt (g)[C]	LVAW (mm)	LVPW (mm)	LVDD (mm)	LVSD (mm)	LVFS (%)	HR (bpm)
<3 days							
+/+	1.73 ± 0.35	0.21 ± 0.01	0.21 ± 0.02	1.58 ± 0.07	1.12 ± 0.10	29 ± 4	346 ± 17
t/t	1.24 ± 0.15	0.14 ± 0.02	0.14 ± 0.02	1.67 ± 0.28	1.41 ± 0.31	16 ± 5	381 ± 43
P[B]	0.002	NS	NS	<0.001	<0.001	0.001	NS
3 weeks							
+/+	16.03 ± 1.45	0.86 ± 0.04	0.81 ± 0.07	2.76 ± 0.03	1.45 ± 0.15	47 ± 6	460 ± 86
t/t	14.60 ± 1.00	1.02 ± 0.13	1.00 ± 0.10	3.42 ± 0.37	2.57 ± 0.48	25 ± 6	458 ± 18
P	NS	NS	0.05	0.04	0.02	0.009	NS
8 weeks							
+/+	22.10 ± 2.21	0.84 ± 0.03	0.82 ± 0.03	2.74 ± 0.43	1.54 ± 0.35	44 ± 6	470 ± 95
t/t	22.99 ± 2.59	1.12 ± 0.13	1.10 ± 0.13	3.56 ± 0.53	2.64 ± 0.46	26 ± 5	414 ± 40
P	NS	<0.001	<0.001	0.006	<0.001	<0.001	NS

[A]Number of animals and age at study: 4 +/+ and 11 t/t (<3 days); 3 +/+ and 3 t/t (3 weeks); 6 +/+ and 10 t/t (8 weeks). Homozygous MyBP-C(Neo) and MyBP-C(LoxP) mice were indistinguishable, and these data (indicated as t/t) reflect measurements made on both types of mutant mice. [B]*P*-value (wild-type vs. mutant MyBP-C mice) derived by Student's unpaired *t* test after raw data were corrected for body weight. [C]Average body weight of mice.

Table 2
Cardiac function of 12-week-old mice assessed by in vivo cardiac catheterization

Cardiac function	Wild-type (+/+)[A]	MyBP-C$^{t/t}$	*P*-value[B]
Stroke work$_{(end\ diastolic\ volume)}$ ($SW_{(EDV)}$) (mmHg)	104.99 ± 7.23	56.30 ± 8.87	0.004
End systolic pressure (mmHg)	100.11 ± 3.49	90.94 ± 7.43	NS
dP/dt_{max} (mmHg/s)	11536.96 ± 852.22	10841.40 ± 794.17	NS
Normalized end-systolic elastance (mmHg/μl*100mg)	13.14 ± 3.38	3.53 ± 0.42	0.02
dP/dt_{min} (mmHg/s)	–9615.07 ± 488.19	–4841.86 ± 223.91	0.0001
dP/dt_{max} / dP/dt_{min}	1.21 ± 0.10	2.25 ± 0.15	0.004
End diastolic pressure (mmHg)	3.28 ± 0.72	3.73 ± 0.58	NS
Time to peak filling (ms)	33.25 ± 1.46	42.70 ± 2.99	0.03
tau (ms)	9.03 ± 0.62	14.56 ± 1.28	0.008
Normalized beta (mmHg/μL^{-1}/100 mg)	0.07 ± 0.01	0.03 ± 0.01	0.01
Heart rate (min^{-1})	601.70 ± 19.65	580.20 ± 21.55	NS

[A]10 wild-type and 5 homozygous mutant MyBP-C(Neo) or MyBP-C(LoxP) mice (designated MyBP-C$^{t/t}$). [B]*P*-value (+/+ vs. t/t) derived by Student's unpaired *t* test.

Protein fractions were separated by standard methods on 6% polyacrylamide mini gels (Western blot analyses), 6% polyacrylamide slab gels (cardiac α- and β-myosin heavy chain [MHC] isoforms; ref. 25), or 12% polyacrylamide slab gels (total proteins). Protein concentration was determined using the Bradford protein assay. The proportion of cardiac α- and β-MHC was quantified by densitometry and NIH-Image software (National Institutes of Health, Bethesda, Maryland, USA).

MyBP-C was identified by Western blot analyses (Amersham Pharmacia Biotech UK, Little Chalfont, Buckinghamshire, England; ref. 26) of total protein or myofibrillar homogenates separated by SDS-PAGE gels (125 V for 2 hours), transferred to a nitrocellulose membranes (35 V for 2.5 hours), and incubated with rabbit anti-chicken skeletal muscle MyBP-C γ-serum polyclonal antibody (diluted 1:10,000; ref. 27). Antibody-labeled proteins were detected using an enhanced chemiluminescence plus kit (ECL+Plus; Amersham Life Sciences Inc.). The relative amounts of antibody-labeled protein were quantified by densitometry and NIH-Image software.

Morphology and microscopy. Animals were sacrificed by cervical dislocation and hearts were excised, rinsed in PBS (GIBCO), and weighed. Cardiac tissues were isolated as described (28) and pathologic evaluations were performed by an experienced cardiac pathologist.

Excised tissues were mounted in paraffin blocks as described (25) and 3–7-μM sections were stained with hematoxylin and eosin (H&E) or Masson trichrome (American HistoLabs Inc. Gaithersburg, Maryland, USA). High-magnification images were obtained using a Zeiss Axiophot light microscope (Carl Zeiss Inc., Thornwood, New York, USA) equipped with a ×2.5, ×20, and ×40 oil immersion objective and a Sony digital photo camera (DKC-5000; Sony Corp., Tokyo, Japan). Images were viewed using Adobe Illustrator software (Adobe Systems Inc., Mountain View, California, USA).

LV and RV sections were prepared for transmission electron microscopy as described previously (29). In brief, sections were fixed with 2.5% glutaraldehyde + 2% paraformaldehyde in 0.1 M cacodylate buffer, pH 7.4, then rinsed 3 times in 0.1 M cacodylate buffer, pH 7.4, and post-fixed in 1% osmium tetroxide (OsO_4) for 2 hours, rinsed in dH_20, and then 1% uranyl acetate for 1 hour (en-block staining). The fixed pellets were dehydrated in alcohol, rinsed twice in propylene oxide for 20 minutes, and embedded overnight with a 1:1 ratio of propylene oxide to Spurr's resin solution. After 12 hours, this solution was replaced with 100% Spurr's solution and then polymerized in a dry oven at 70°C for 48 hours. Ultrathin sections (100-nm thick) from the stained and embedded samples were observed in transmission mode using a Phillips CM12 electron microscope (FEI Company, http://www.feic.com).

Assessment of LV function. Transthoracic echocardiography was performed in 0 to 3 day-old mice using a high-frequency (45 MHz) echocardiographic technique (25). Echocardiographic imaging was performed without anesthesia and with mice lightly restrained in a supine position using a Humphrey Ultrasound Biomicroscope (model 840; Humphrey Instruments, San Leandro, California, USA). LV parameters were obtained from the 2-dimensional echocardiographic images in a short-axis view. Neonatal mouse heart rates were determined from continuous-wave Doppler tracing using a high-frequency Doppler system (25, 30).

Transthoracic echocardiography was performed in adult mice (> 3 weeks old) using a Sonos 5500 ultrasonograph with a 12-MHz transducer (Hewlett-Packard, Andover, Massachusetts, USA). Mice were anesthetized with 2.5% Avertin (0.010 mL/g) and warmed with a heating pad during echocardiographic examination. Two-dimensional echocardiographic images were obtained with mice orientated in a left lateral decubitus or supine position. LV parameters were obtained from M-mode interrogation in a short-axis view. Orthogonal left atrial diameter (LAD) was obtained from 2-dimensional echocardiographic images in a long-axis view. Echocardiographic measurements, for both neonatal and adult mouse studies, were averaged from at least 3 separate cardiac cycles: LV anterior wall (LVAW) thickness, LV posterior wall (LVPW) thickness, maximal LV diastolic diameter (LVDD), minimum LV systolic diameter (LVSD), LV fractional shortening (LVFS), maximal LAD, and heart rate. The statistical significance of differences in echocardiographic parameters between wild-type and MyBP-C mice was determined by unpaired Student's *t*-test. Data are expressed as mean ± SD. A *P* value less than 0.05 was considered significant.

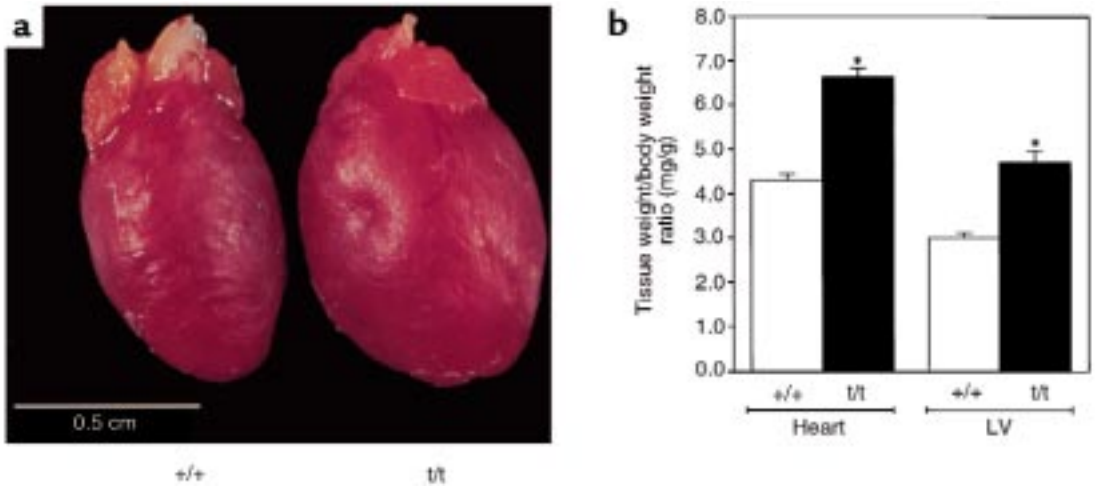

Figure 3
Comparison of hearts from 8–12-week-old wild-type and homozygous mutant mice. (**a**) Gross morphology of homozygous MyBP-C(Neo) (designated t/t) and wild-type (+/+) hearts and (**b**) heart-to-body weight or LV-to-body weight ratios demonstrate significant increases ($P < 0.001$) in cardiac size of homozygous mutant mice (t/t) versus wild-type mice (+/+).

Analysis of LV-chamber systolic and diastolic properties was performed in vivo as described (31). In brief, a miniaturized impedance/micromanometer catheter was used to derive real-time LV pressure-volume relationships. Animals were anesthetized with etomidate (10–20 mg/kg body weight), morphine (1–2 mg/kg body weight), and urethane (750 mg/kg body weight), intubated, and artificially ventilated with a custom-designed murine ventilator, with 100% inspired oxygen at a tidal volume of 200 μL and frequency of 120 breaths per minute. Heart rates were near normal (>500 beats per minute). The LV was catheterized using an apical stab exposed by a limited thoracotomy. Signals were recorded at steady state and during transient load reduction produced by transiently occluding the inferior vena cava. Data were sampled at 2 kHz and analyzed with custom software. Following initial data collection, an ultrasound perivascular flow probe (1RB; Transonics, Ithaca, New York, USA) was placed around the thoracic aorta to measure cardiac output. The stroke volume was used to calibrate relative volumes measured simultaneously by the volume-catheter signal, matching its value to the mean width of the pressure-volume loop. Relative changes and the majority of derived hemodynamic parameters were calibrated, although absolute volume was not. Heart weights and gross anatomic examinations were made after completion of each study. Comparisons between wild-type and mutant MyBP-C mice were performed by Student *t* tests. All data are reported as means ± SEM and *P* values less than 0.05 are numerically reported; higher values are indicated as nonsignificant.

Results

Construction MyBP-C(Neo) and MyBP-C(LoxP) alleles. A segment of the murine MyBP-C gene was isolated from a bacteriophage λDASH genomic library and its nucleotide sequence determined (unpublished). Exons 29–31 were identified on a 7.4-kb *Spe*I fragment that was subcloned; the neomycin resistance gene (*PGK-Neo-polyA*) flanked by LoxP sequences was inserted into exon 30 (Figure 1a and Methods). This construct was used to disrupt the endogenous MyBP-C gene in ES cells by homologous recombination and the targeted allele was designated *MyBP-C(Neo)*. Blastocysts injected with ES cells bearing the *MyBP-C(Neo)* allele produced chimeric animals. The amount of mutant MyBP-C mRNA in cardiac tissues from mice bearing this allele was significantly less than the amount of MyBP-C mRNA found in wild-type mice (see below). We hypothesized that the amount of mutant MyBP-C mRNA was reduced because the neomycin-resistant gene sequences in the mutant mRNA caused the RNA to be degraded rapidly or because these sequences altered the processing of MyBp-C RNA precursor. To test this hypothesis, a second allele, designated *MyBP-C(LoxP)*, was created by mating chimeric MyBP-C(Neo) mice with a transgenic mouse expressing CRE. The *MyBP-C(LoxP)* allele resulted from excision of the neomycin resistance gene by CRE recombinase and contains a residual 97-bp duplicated LoxP sequence (Figure 1a and data not shown). Heterozygous offspring of chimeric animals were bred to produce mice homozygous for either the *MyBP-C(Neo)* or *MyBP-C(LoxP)* allele. Mice homozygous for each allele were characterized by Southern blot analyses and by PCR amplification of the *MyBP-C(LoxP)* allele with primers 1F,1R (Figure 1a) and the *MyBP-C(Neo)* allele with primers 1F,3R and 2F,2R (Figure 1a; data not shown). Homozygous MyBP-C(Neo) and MyBP-C(LoxP) mice were fertile, produced normal litter sizes, and survived more than 1 year.

Cardiac MyBP-C mRNA and protein expression from mutant MyBP-C alleles. The amounts of cardiac MyBP-C mRNA in MyBP-C(LoxP) and MyBP-C(Neo) mouse hearts were assessed by Northern blot analyses. The abundant cardiac MyBP-C transcripts (4.5 kb) found in wild-type mice were markedly reduced in the LV (14.5

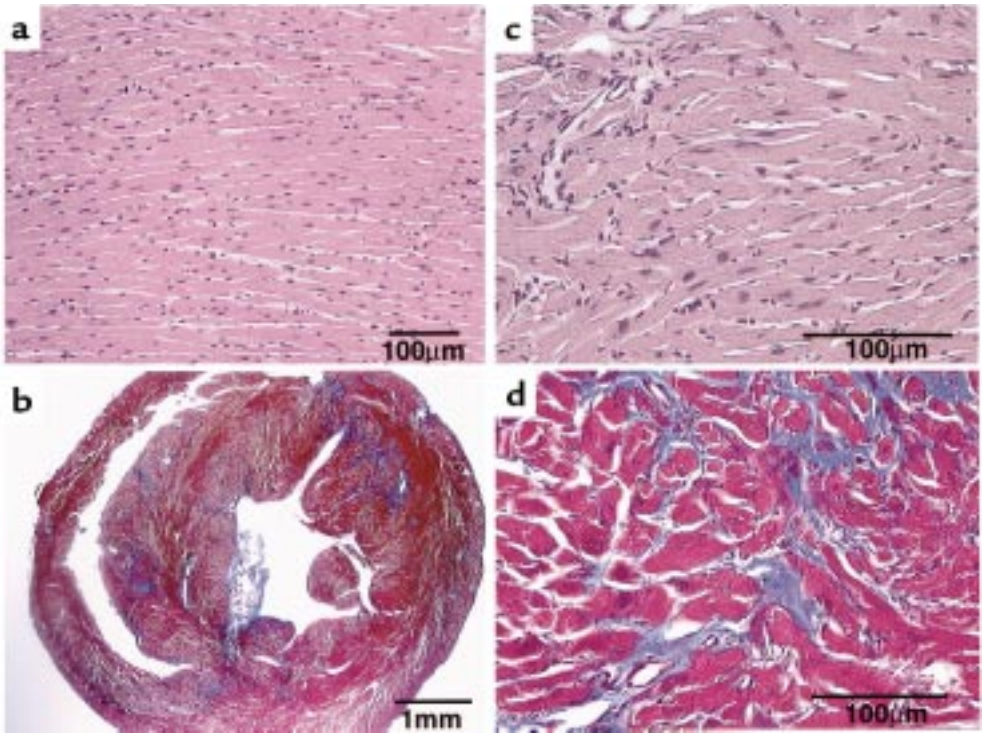

Figure 4
Histology of 8–12-week-old wild-type (**a**) and MyBP-C(Neo) (**b**–**d**) mouse hearts. Sections were stained with H&E (**a** and **c**) or Masson trichrome (**b** and **d**).

± 4%; *n* = 6), RV (9.5 ± 1%; *n* = 3), and atria (18.4 ± 5%; *n* = 3) of MyBP-C(Neo) mice (Figure 2a and data not shown). Cardiac tissues from MyBP-C(Neo) mice and MyBP-C(LoxP) mice contained approximately the same amount of cardiac MyBP-C mRNA (data not shown).

The structure of the cardiac MyBP-C RNA produced from each allele was characterized by nucleotide sequence analyses of RT-PCR–amplified products derived from homozygous mutant mouse heart total RNA (see Methods). The structures of the cardiac MyBP-C sequences found in the hearts of the mutant mice were compared with wild-type RNA sequences and were consistent with the model that the different mutant RNAs resulted from alternate splice patterns (Figure 1, a and b). That is, RNA derived from the *MyBP-C(Neo)* allele spliced out exon 30 whereas RNA derived from the *MyBP-C(LoxP)* allele lacked the 5′ part of exon 30 because the RNA was spliced from the 3′ end of exon 29 to the LoxP sequence (Figure 1). The predicted mutant MyBP-C polypeptides encoded by the altered MyBP-C alleles differ at their carboxyl termini (Figure 1b). The *MyBP-C(LoxP)* allele produces a protein that has 166 novel amino acid residues and is 30 residues shorter than the wild-type protein, whereas the MyBP-C(Neo) protein is 174 amino acid residues shorter than the wild-type protein and has 32 novel amino acid residues (Figure 1b).

The amount of mutant peptide found in the ventricles of homozygous mutant MyBP-C mice was assessed by Western blot analyses. Polyclonal MyBP-C antibodies identified a 150-kDa protein in LV total protein and myofibrillar-enriched protein preparations that comigrated with chicken MyBP-C (Figure 2b and data not shown). Although the mutant protein from MyBP-C(Neo) mice was theoretically 15 kDa smaller than wild-type MyBP-C protein, the mutant and wild-type proteins migrated at approximately the same position on a 6% SDS-PAGE gel. (Why the smaller mutant peptide comigrated with the large wild-type protein is uncertain.). Mutant cardiac MyBP-C protein in total protein homogenates of the LV from MyBP-C(Neo) mice was 2.3 ± 1% (*n* = 6), the amount found in analogous wild-type extracts (data not shown). Myofibrillar extracts contained significantly more mutant peptide than corresponding amounts of total protein extract. Mutant cardiac MyBP-C protein levels in myofibrillar extracts were 9.5 ± 3 % (*n* = 8) the amount of MyBP-C in wild-type myofibrillar extracts (Figure 2b). Similar analyses demonstrated that the MyBP-C(LoxP) mutant protein was also enriched in the myofibrillar fraction compared with the amount in the total cytoplasmic fraction (data not shown).

Cardiac morphology of homozygous mutant MyBP-C mice. Cardiac structure was characterized in mutant MyBP-C mice at 8–12 weeks of age. Hearts from both homozygous MyBP-C(Neo) and homozygous MyBP-C(LoxP) mutant mice were visibly enlarged compared with those from wild-type mice, and calcified plaques were present on the LV chamber walls of homozygous mutant MyBP-C mouse hearts but not wild-type mice (Figure 3 and data not shown). Total heart weights in mutant versus wild-type animals (177.0 ± 5.7 mg, *n* = 26 vs. 113.8 ± 3.8 mg, *n* = 25) and LV weights (136.0 ± 7.5 mg, *n* = 12, vs.

80.0 ± 4.8 mg, n = 11) were significantly increased (P < 0.001). Heart-to-body weights and LV-to-body weight ratios were also greater in mutant MyBP-C mice than in wild-type mice (Figure 3b). In contrast, RV left and right atria were of comparable size and weights in mutant and wild-type mice (Figure 3 and data not shown).

Both homozygous MyBP-C(Neo) and MyBP-C(LoxP) hearts demonstrated prominent histologic abnormalities, including myocyte hypertrophy, myofibrillar disarray, and fibrosis. In addition 3 of 5 mutant hearts had dystrophic calcification (Figure 4, b and d), which varied in extent and location. Focal LV and RV calcifications and multifocal intramural calcification were found in 2 of 5 hearts, as well as subendocardial calcification with multifocal interstitial fibrosis (1 of 5 hearts), and subendocardial papillary muscle with slight perivascular fibrosis (1 of 5 hearts).

Sarcomeres from homozygous mutant MyBP-C(Neo) mouse hearts were examined by electron microscopy (Figure 5) The sarcomeres of these mouse hearts were well-organized with regularly aligned A-bands, I-bands, and Z-lines; the spacing of these bands was similar to that observed in sarcomeres from wild-type mice. The M-line was frequently absent in sarcomeres from the LV of homozygous MyBP-C mice (Figure 5), however in sarcomeres derived from the RV, well-defined M-lines were found (data not shown).

Cardiac function of homozygous mice bearing mutant MyBP-C alleles. Cardiac function was assessed in adult and neonatal homozygous MyBP-C(Neo) mice using transthoracic echocardiography (Figure 6, a–c, and data not shown; see Methods). At birth (0–3 days) and throughout adulthood (from 3 weeks after birth), mutant MyBP-C mouse hearts demonstrated increased LV diastolic and systolic diameter as well as reduced LV fractional shortening (Table 1). LV wall thickness was used to assess whether ventricular hypertrophy was present. In the neonatal period, anterior and posterior LV wall thickness in homozygous mutant MyBP-C mice was not significantly different from the wall thickness of wild-type mice after correction for body weight differences (Table 1). As wild-type and mutant mice aged, LV wall thickness increased; however, this increase was greater in homozygous mutant MyBP-C mice, and by 8 weeks of age mutant mice had significantly thicker LV walls than did wild-type mice (Table 1). LAD of homozygous mutant MyBP-C mice were also significantly increased in comparison with wild-type mice (1.77 ± 0.13 mm vs. 1.53 ± 0.08 mm; P = 0.01) at 8–12 weeks of age. Echo-dense material, consistent with calcification of the papillary muscles and focal lesions within the LV, was observed in all (10 of 10) homozygous mutant MyBP-C mice at 8 weeks; in 6 animals these changes were moderate to severe.

Cardiac function of homozygous MyBP-C(Neo) mice was further assessed in anesthetized mice by in vivo catheterization (31). Pressure-volume loops obtained from homozygous MyBP-C(Neo) mice and wild-type mice demonstrated significant differences between the cardiac function of these 2 strains (Figure 6d). Although the isovolumic phase of systole was normal, abnormalities were evident with the onset of contraction, consistent with abnormal fractional shortening observed in echocardiographic studies. The abnormal profile of systolic contraction was reflected in several quantitative parameters (Table 2). Diastolic properties (dP/dT_{min}, dP/dT_{ratio}, end-diastolic volume ($SW_{(EDV)}$), time to peak filling, relaxation time (tau), and chamber compliance (normalized beta) were abnormal. Heart rates, dP/dT_{max}, end-diastolic pressure, and end-systolic pressure were not different between mutant and wild-type mice.

RNA and protein expression associated with cardiomyopathy. Altered gene expression, a recognized feature of dilated cardiomyopathy (reviewed in refs. 32, 33), was examined in homozygous mutant MyBP-C(Neo) and MyBP-C(LoxP) mice. Mutant mice expressed α-skeletal actin at levels 16- and 8-fold above that found in

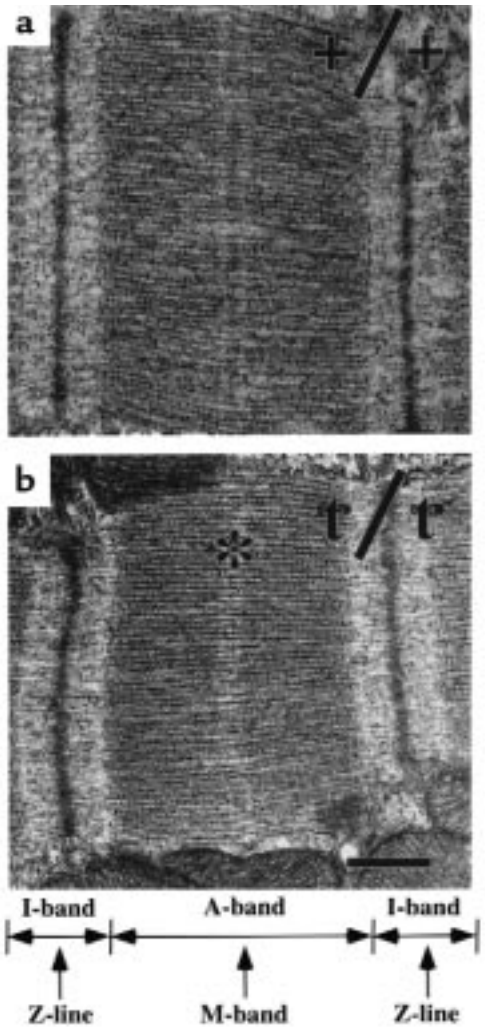

Figure 5
Transmission electron micrographs of sarcomeres from 12-week-old wild-type (**a**) and MyBP-C(Neo) mouse hearts (t/t). Note the unusual appearance of the M-line (asterisk) in MyBP-C(Neo) mouse-derived sarcomeres. Bar, 0.5 μm.

LV and RV tissues from wild-type mice (Figure 7a). Atrial expression of α-skeletal actin was similar in mutant and wild-type animals. Brain natriuretic peptide (BNP) expression was increased 5.3- and 2.2-fold in the LV and RV of homozygous mutant MyBP-C(Neo) mice, compared with wild-type mice, respectively, but expression in atrial tissues was not significantly different.

Expression of α and β cardiac MHC isoforms is altered in many models of dilated cardiomyopathy. The predominant (85%) isoform in LV from wild-type mice is α-MHC, whereas only 15% is β-MHC (25) (Figure 7b). Homozygous mutant MyBP-C LV tissues had significantly increased expression of β-MHC (48%), whereas expression of the α-MHC isoform was reduced to 52%.

To determine whether proteins that regulate myocyte Ca^{2+} cycling were altered in homozygous mutant mouse myocardium, we measured sarcoplasmic reticulum Ca^{2+}-ATPase (SERCA) RNA levels. No differences were observed in SERCA mRNA levels in the LV, RV, or atrium of wild-type and homozygous mutant mice (data not shown).

Discussion

We have produced 2 strains of mice bearing mutant alleles of the cardiac MyBP-C gene. Homozygous mice bearing these alleles have reduced levels (< 10% normal) of mutationally altered MyBP-C peptides expressed in cardiac tissue. The altered peptides are shorter than wild-type MyBP-C and have novel sequences at their carboxyl termini (Figure 1b). The mutant mouse allele *MyBP-C(Neo)* described here encodes an altered peptide similar to mutant peptides found in some individuals with FHC (Figure 1b and Family NN in ref. 3). Both the Family NN mutation and the *MyBP-C(Neo)* allele produce MyBP-C RNA lacking exon 30 because the precursor RNA splices from exon 29 to exon 31 (Figure 1a). The alternate splice creates a frameshift causing the mutant RNA to encode a truncated protein (Figure 1b). Heterozygous humans or mice bearing these mutations develop hypertrophy cardiomyopathy. However, echocardiography and in vivo cardiac catheterization demonstrate that the functional consequence of homozygous mutant MyBP-C alleles is dilated cardiomyopathy. Homozygous mice bearing the mutant MyBP-C alleles have ventricular dysfunction at birth, which continues throughout life and is accompanied by progressive compensatory LV hypertrophy. Histologic manifestations of disease include prominent myocyte hypertrophy, myofibrillar disarray, fibrosis, and dystrophic calcification. Altered gene expression in cardiac tissue from homozygous mutant mice is typical of patterns found in other models of dilated cardiomyopathy (32, 33): α-skeletal actin and BNP mRNAs are found at high levels and myosin isoform expression is altered. These studies provide insights into the normal function of MyBP-C, the mechanism by which mutations in this peptide causes human dis-

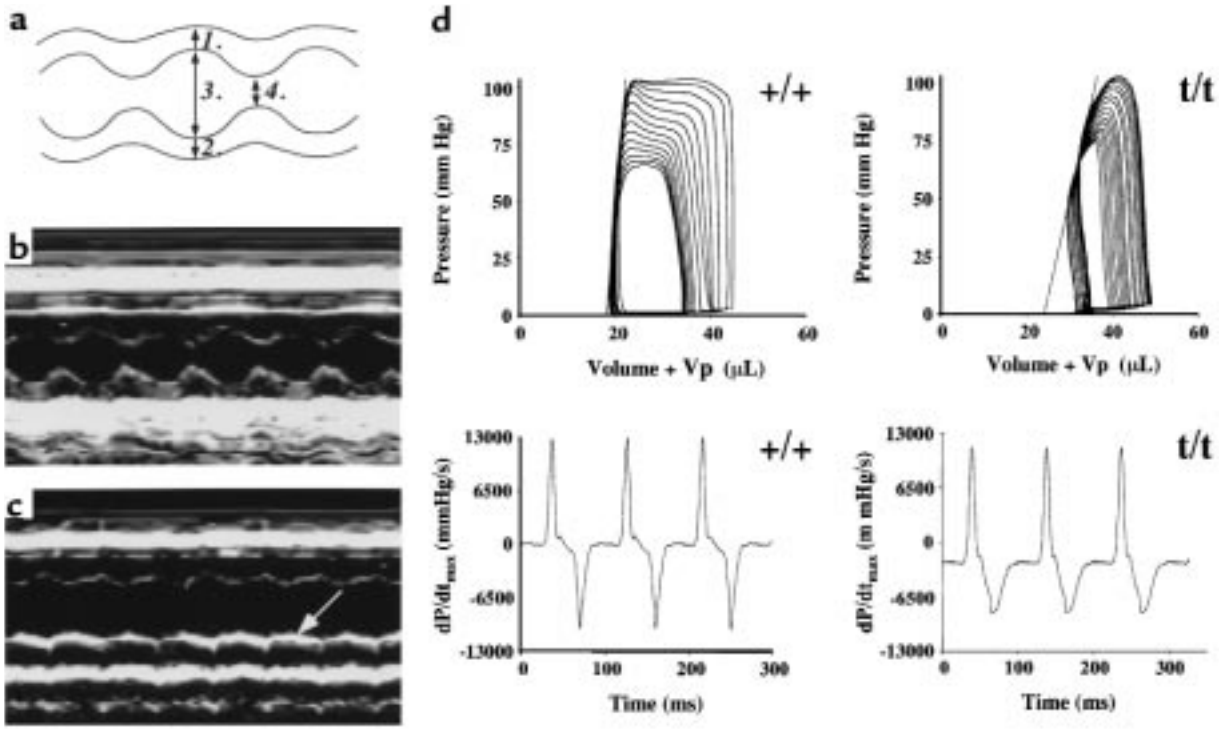

Figure 6

Cardiac function in wild-type and MyBP-C(Neo) mice. (**a**–**c**) Schematic and M-mode echocardiographic tracings from 12-week-old wild-type (**b**) and MyBP-C(Neo) mice (**c**). LV dimensions are calculated from measurements of anterior wall (1), posterior wall (2), end-diastolic diameter (3), and end-systolic diameter (4). Increased contrast in the posterior papillary muscle probably reflects calcification (**c**) (arrow). (**d**) Pressure volume relations and dP/dt profiles of wild-type (+/+) and MyBP-C(Neo) mice (t/t).

ease, and further indicate a molecular relatedness of hypertrophic and dilated cardiomyopathy.

During embryogenesis, appearance of MyBP-C correlates with the appearance of cross striations (13), implying a developmental role for this molecule in alignment of thick filaments within the sarcomeres. Because the mutated MyBP-C alleles described here encode truncated peptide sequences that participate in binding myosin and the level of foreshortened peptide is markedly less than normal MyBP-C, we were particularly surprised to find near-normal sarcomeres in mutant hearts. Neither the banding patterns nor the length of sarcomeres were adversely affected by MyBP-C deficits. These data either imply a nonessential role for MyBP-C in forming and maintaining sarcomere ultrastructure or, alternatively, indicate that other molecules (possibly MyBP-H) can substitute for these MyBP-C functions. In any event, MyBP-C is not required in stoichiometric quantities to produce normal looking sarcomeres.

Transmission electron microscopy of LV tissues from homozygous mice bearing mutant MyBP-C alleles showed that the M-band was often less distinct and nonhomogenous compared with that found in wild-type specimens. M-bands are primarily composed of the thick filament–associated components, MyBP-C, M-protein, skelemin, and myomesin. MyBP-C normally forms 7 to 9 stripes in the C-zone of the A-band, on either side of the M-band (11–13, 34). Whereas the poorly defined M-bands in LV from homozygous mutant mouse hearts could reflect altered composition of these MyBP-C stripes, several findings indicate this abnormal pattern is a consequence of the cardiac dysfunction evident in mutant mice. First, equivalent levels of mutant peptide were found in both ventricular chambers; however, all M-bands in the RV (and some LV M-bands) of mutant animals appeared normal, implying that hemodynamic forces influence this banding pattern. Second, indistinct LV M-bands have also been observed in mice overexpressing tropomodulin, a thin filament component (35). Since both tropomodulin transgenics and homozygous mutant MyBP-C mice develop dilated cardiomyopathy, we suggest that M-band loss within the LV is a consequence rather than cause of sarcomere dysfunction.

Heterozygous humans bearing cardiac MyBP-C gene mutations that encode truncated polypeptides develop hypertrophic cardiomyopathy. The mechanism by which these cause disease is unclear because neither mutant MyBP-C peptides nor reduced peptide levels were found in myofibrillar fractions prepared from cardiac tissues of an affected individual (18). Transgenic mice have recently been reported to express mutant cardiac MyBP-C under the α-MHC promoter (36), but levels were so robust as to diminish endogenous wild-type MyBP-C gene expression. Homozygous mice bearing mutant MyBP-C alleles provide evidence that mutated MyBP-C genes that are regulated by the endogenous promoter produce mutant peptides that appear to be incorporated into sarcomeres. That is, 4-fold more mutant peptide was found in myofibrillar extracts than total cell extracts of LV tissue (see Figure 2b and Results). Extension of these findings to humans carrying analogous cardiac MyBP-C gene defects suggests that hypertrophic cardiomyopathy is caused by the dominant negative action of mutant MyBP-C peptide on sarcomere function, although the possibility that reduction in the amount of MyBP-C has a role in the disease process has not been excluded.

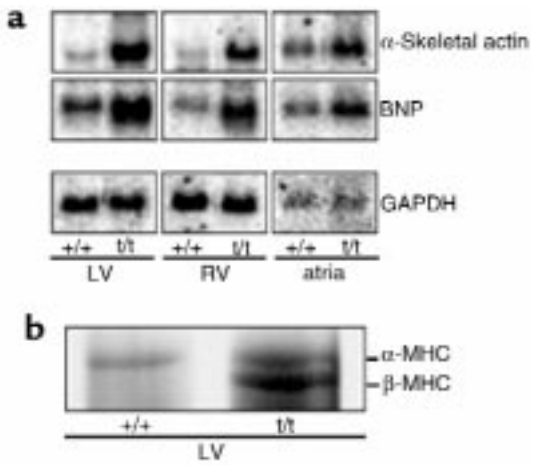

Figure 7
Altered gene expression in hearts from MyBP-C(Neo) mice. Northern blots (**a**) show increased expression of α-skeletal actin and BNP mRNAs in comparison with GAPDH transcripts. Silver-stained SDS-page gels (**b**) demonstrate altered expression of cardiac MHC isoforms in total ventricular extracts from MyBP-C(Neo) mouse hearts (from 8–12-week-old animals; designated t/t) compared with protein from wild-type mice (+/+).

Mice expressing homozygous sarcomere gene defects may help to address another aspect of human hypertrophic cardiomyopathy. Analyses of phenotype and genotype in this disorder have demonstrated the influence that genetic etiology has on survival in affected individuals (for reviews see ref. 8, 9). Although genetically engineered mice that are heterozygous for a human gene mutation have provided important reagents for dissecting the biology of this disease, the natural history of disease in these models has not been useful in defining mutations that cause premature death in humans. For example, individuals with the myosin mutation *Arg403Gln* have markedly shortened life expectancies, whereas mice with the comparable mutation (designated $\alpha\text{-MHC}^{403/+}$) have normal survival. In contrast, survival in 3 lines of mice that are homozygous for human hypertrophic mutations more precisely mimicked the premature death observed in humans with the corresponding mutations: survival is markedly reduced in $\alpha\text{-MHC}^{403/403}$ mice but near-normal in homozygous mice bearing mutant MyBP-C alleles. Whereas study of other hypertrophic cardiomyopathy mutations is needed to validate these observations, we suggest that homozy-

gous murine models may be valuable reagents for profiling survival, particularly because relevant clinical information from humans who share a mutation is often unavailable.

An important question resulting from these studies is how a 2-fold difference in the amount of mutant sarcomere proteins causes markedly different phenotypes: hypertrophy versus dilation. That is, heterozygous mice bearing sarcomere protein gene mutations develop hypertrophic cardiomyopathy whereas homozygous mutant mice bearing the same mutations develop dilated cardiomyopathy. We hypothesize that parameters of sarcomere function, such as force generation, are monitored and serve as the central signaling mechanism that triggers different pathways to remodel the heart. When force produced by an admixture of mutant and normal sarcomere proteins is sufficiently impaired, compensatory myocyte growth occurs, resulting in cardiac hypertrophy. However, when sarcomere function remains inadequate despite growth (as in α-MHC$^{403/403}$ and homozygous mutant MyBP-C hearts), other pathways are activated, as evidenced by altered gene expression (e.g., α-skeletal actin, BNP, and β-MHC), myocyte death, and fibrosis. If severity of sarcomere dysfunction is the central signal relating these pathways, then an extension of this model predicts that external forces on the myocyte, such as hemodynamic load or extracellular matrix remodeling, could exacerbate intrinsic sarcomere dysfunction and tip the balance from compensated hypertrophy toward uncompensated failure. This mechanism could account for progression of hypertrophic to dilated cardiomyopathy

Acknowledgments

We would like to thank Michael Giewat and John Gabrovsek for technical assistance. This research was supported by the Howard Hughes Medical Institute.

1. Chien, K.R., Grace, A.A., and Hunter, J.J. 1999. Molecular and cellular biology of cardiac hypertrophy and failure. In *Molecular basis of cardiovascular disease*. K.R. Chien, editor. W.B. Saunders Co. Philadelphia, PA. 251–264.
2. Rodkey, S.M., Ratliff, N.B., and Young, J.B. 1998. Cardiomyopathy and myocardial failure. In *Comprehensive cardiovascular medicine.* E.J. Topal, editor. Lippincott-Raven Publishers. Philadelphia, PA. 2589–2620.
3. Watkins, H., et al. 1995. Mutations in the cardiac myosin binding protein C gene on chromosome 11 cause familial hypertrophic cardiomyopathy. *Nat. Genet.* **11**: 434–437.
4. Bonne, G., et al. 1995. Cardiac myosin binding protein-C gene splice acceptor site mutation is associated with familial hypertrophic cardiomyopathy. *Nat. Genet.* **11**:438–440.
5. Niimura, H., et al. 1998. Mutations in the gene for cardiac myosin-binding protein C and late-onset familial hypertrophic cardiomyopathy. *N. Engl. J. Med.* **338**:1248–1257.
6. Bonne, G., Carrier, L., Richard, P., Hainque, B., and Schwartz, K. 1998. Familial hypertrophic cardiomyopathy: from mutations of functional defects. *Circ. Res.* **83**:580–593.
7. Carrier, L., et al. 1997. Organization and sequence of human cardiac myosin binding protein C gene (MYBPC3) and identification of mutations predicted to produce truncated proteins in familial hypertrophic cardiomyopathy. *Circ. Res.* **80**:427–434.
8. Seidman, C.E., and Seidman, J.G. 1997. Gene defects that cause inherited cardiomyopathy. In *Molecular basis of heart disease.* K.R. Chien, J.L. Breslow, J.M. Leiden, R.D. Rosenberg, and C.E. Seidman, editors. W.B. Saunders. Philadelphia, PA. pp. 251–263.
9. Seidman, C.E., and Seidman, J.G. 1998. Molecular genetic studies of familial hypertrophic cardiomyopathy. *Basic Res. Cardiol.* **93**(Suppl.):13–16.
10. Gruen, M., and Gautel, M. 1999. Mutations in beta-myosin S2 that cause familial hypertrophic cardiomyopathy (FHC) abolish the interaction with the regulatory domain of myosin binding protein-C. *J. Mol. Biol.* **286**:933–949.
11. Dennis, J., Shimizu, E.T., Reinach, F.C., and Fischman, D.A. 1984. Localization of C-protein isoforms in chicken skeletal muscle: ultrastructural detection using monoclonal antibodies. *J. Cell Biol.* **98**:1514–1522.
12. Bennett, P., Craig, R., Starr, R., and Offer, G. 1986. The ultrastructural location of C-protein, X-protein and H-protein in rabbit muscle. *J. Muscle Res. Cell. Motil.* **7**:550–567.
13. Seiler, S.H., Fischman, D.A., and Leinwand, L.A. 1995. Modulation of myosin filament organization by C-protein family members. *Mol. Biol. Cell.* **7**:113–127.
14. Gautel, M., Suffardi, O., Freiburg, A., and Labeit, S. 1995. Phosphorylation switches specific for the cardiac isoform of myosin binding protein C: a modulator of cardiac contraction? *EMBO J.* **14**:1952–1960.
15. Schlender, K., and Bean, L.J. 1991. Phosphorylation of chick cardiac C-protein by calcium/calmodulin-dependent protein kinase II. *J. Biol. Chem.* **266**:2811–2817.
16. Hartzell, H.C. 1985. Effects of phosphorylated and unphosphorylated C-protein on cardiac actomyosin ATPase. *J. Mol. Biol.* **186**:185–195.
17. Hofmann, P.A., Hartzell, H.C., and Moss, R.L. 1991. Alterations in Ca^{2+} sensitive tension due to partial extraction of C-protein from rat skinned cardiac myocytes and rabbit skeletal muscle fibers Ca^{2+} activation. *J. Gen. Physiol.* **97**:1141–1163.
18. Rottbauer, W., et al. 1997. Novel splice donor site mutations in the cardiac myosin-binding protein-C gene in familial hypertrophic cardiomyopathy: characterization of cardiac transcript and protein. *J. Clin. Invest.* **100**:475–482.
19. Hendrickson, B.A., et al. 1995. Altered hepatic transport of immunoglobulin A in mice lacking the J chain. *J. Exp. Med.* **182**:1905–1911.
20. Ho, C., et al. 1995. A mouse model of human familial hypocalciuric hypercalcemia and neonatal severe hyperparathyroidism. *Nat. Genet.* **11**:389–394.
21. Lakso, M., et al. 1996. Efficient in vivo manipulation of mouse genomic sequences at the zygote stage. *Proc. Natl. Acad. Sci. USA.* **93**:5860–5865.
22. Ogawa, T., et al. 1996. Evidence for load-dependent and load-independent determinants of cardiac natriuretic peptide production. *Circulation.* **93**:2059–2067.
23. Jones, W.K., et al. 1996. Ablation of the murine α myosin heavy chain leads to dosage effects and functional deficits in the heart. *J. Clin. Invest.* **98**:1906–1917.
24. McConnell, B.K., Moravec, C.S., Morano, I., and Bond, M. 1997. Troponin I phosphorylation in spontaneously hypertensive rat hearts: effect of α-adrenergic stimulation. *Am. J. Physiol.* **273**:H1440–H1451.
25. Fatkin, D., et al. 1999. Neonatal cardiomyopathy in mice homozygous for the Arg403Gln mutant in the α-cardiac myosin heavy chain gene. *J. Clin. Invest.* **103**:147–153.
26. McConnell B.K., Moravec, C.S., and Bond, M. 1998. Troponin I phosphorylation and myofilament calcium sensitivity during decompensated cardiac hypertrophy. *Am. J. Physiol.* **274**:H385–H396.
27. Einheber, S., and Fischman, D.A. 1990. Isolation and characterization of a cDNA clone encoding avian skeletal muscle C-protein: an intracellular member of the immunoglobulin superfamily. *Proc. Natl. Acad. Sci. USA.* **87**:2157–2161.
28. Geisterfer-Lowrance, et al. 1996. A mouse model of familial hypertrophic cardiomyopathy. *Science.* **272**:731–734.
29. Di Francesco, A., et al., 1998. Changes in Mg content and subcellular distribution during retinoic acid induced differentiation of HL60 cells. *Arch. Biochem. Biophys.* **360**:149–157.
30. Aristizabal, O., Christopher, D.A., Foster, F.S., and Turnbull, D.H. 1998. 40-MHz echocardiographic scanner for cardiovascular assessment of mouse embryos. *Ultrasound Med. Biol.* **24**:1407–1417.
31. Georgakopoulos, D., et al. 1999. Dissecting the pathogenesis of familial hypertrophic cardiomyopathy: primary and secondary effects of an α-cardiac myosin heavy chain missense mutation. *Nat. Med.* **5**:327–330.
32. Vikstrom, K.L., Bohlmeyer, T., Factor, S.M., and Leinwand, L.A. 1998. Hypertrophy, pathology, and molecular markers of cardiac pathogenesis. *Circ. Res.* **82**:773–778.
33. Kubota, T., et al. 1997. Dilated cardiomyopathy in transgenic mice with cardiac-specific overexpression of tumor necrosis factor-alpha. *Circ. Res.* **81**:627–635.
34. Schiaffino, S., and Reggiani, C. 1996. Molecular diversity of myofibrillar proteins: gene regulation and functional significance. *Physiol. Rev.* **76**:371–423.
35. Sussman, M.A., et al. 1998. Myofibril degeneration caused by tropomodulin overexpression leads to dilated cardiomyopathy in juvenile mice. *J. Clin. Invest.* **101**:51–61.
36. Yang, Q., et al. 1998. A mouse model of myosin binding protein C human familial hypertrophic cardiomyopathy. *J. Clin. Invest.* **102**:1292–1300.